SUPPORTING INFORMATION

Exploiting the Flexibility of the Pyrochlore Composition for Acid-Resilient Iridium Oxide Electrocatalysts in Proton Exchange Membranes

David L. Burnett, Enrico Petrucco, Reza J. Kashtiban, Stewart F. Parker, Jonathan D.B Sharman and R.I. Walton

S1: Thermodiffraction results

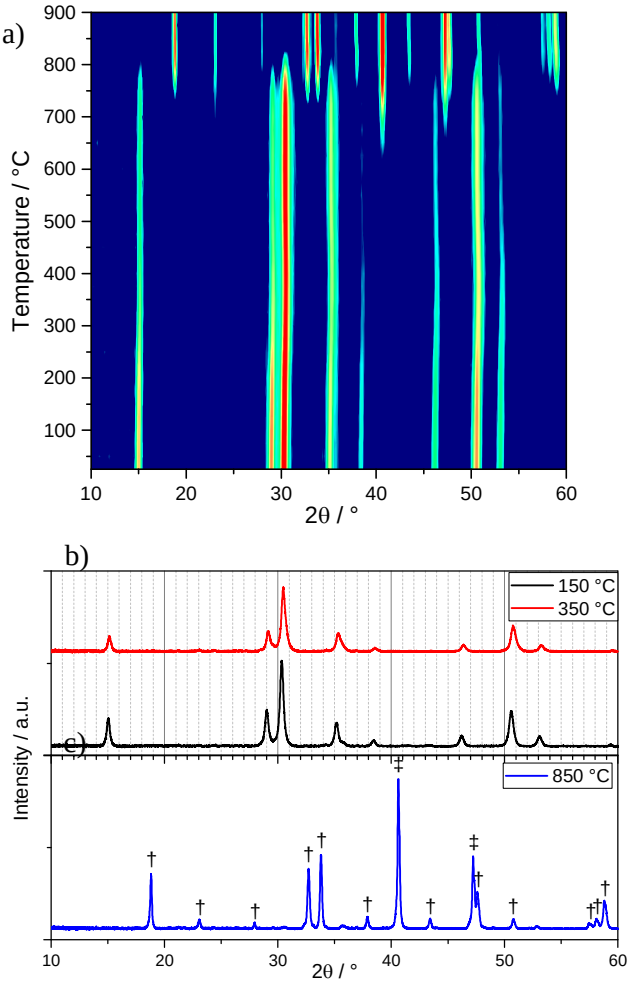

Figure S1.1: a) Thermodiffractometry (λ = 1.5418 Å) of calcium sodium iridium oxide synthesised from CaO_2. b) XRD patterns above and below the temperature at which crystal water is lost. c) XRD pattern after structure collapse, † denotes peaks arising from Ca_2IrO_4 and ‡ denoting peaks arising from Ir metal.

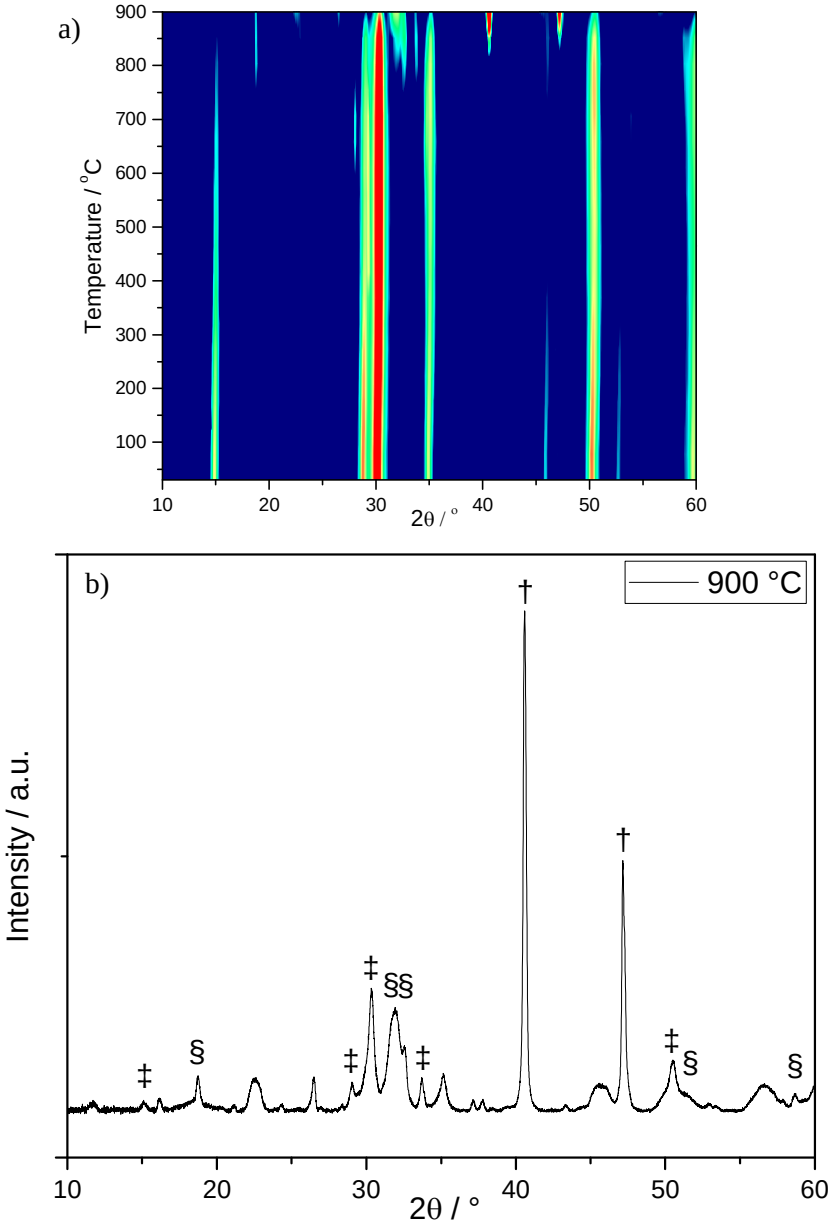

Figure S2.2: a) Thermodiffractometry (λ = 1.5418 Å) of calcium iridium oxide. b) XRD pattern at 900 °C, † denoting peaks arising from Ir metal, ‡ denoting peaks arising from possible pyrochlore phase and § denoting peaks from possible Ca_2IrO_4 phase

S2: Characterisation of B-site substituted materials

S2.1 Antimony substitution

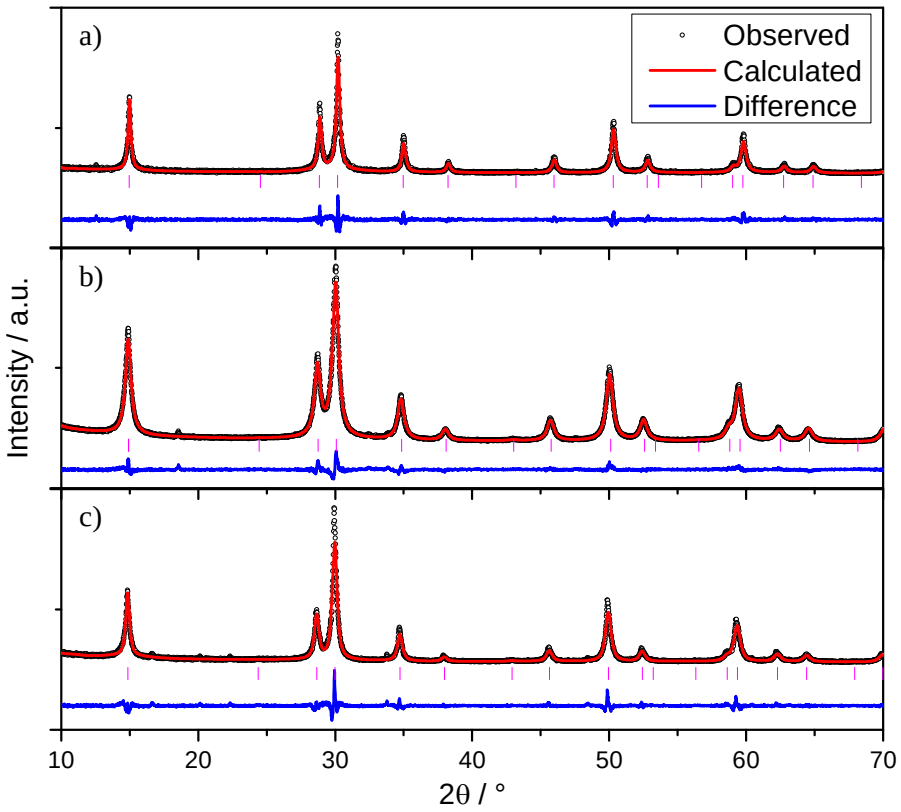

Figure S2.1.1: Rietveld refinements against powder XRD data (λ = 1.54056 Å) for $(Ca,Na)_{2-x}(Ir_{1-y}Sb_y)_2O_6 \cdot H_2O$, a) y = 0.25, b) y = 0.50 and c) y = 1.00.

Table S2.1.1: Structural details of $(Ca,Na)_{2-x}(Ir_{1-y}Sb_y)_2O_6 \cdot H_2O$ pyrochlores obtained from Rietveld refinement against powder XRD data.

Atom	Site	*x*	*y*	*z*	Occ	U_{iso} / Å^2
25% Sb Pyrochlore: *a* = 10.2561(2) Å / Crystallite Size = 17.8 ± 3.4 nm						
Ca	16*d*	0.5	0.5	0.5	0.666(7)	0.0369(19)
Na	16*d*	0.5	0.5	0.5	0.322(12)	0.0369(19)
Ir	16*c*	0	0	0	0.708(4)	0.0062(3)
Sb	16*c*	0	0	0	0.292(4)	0.0062(3)
O	48*f*	0.3391(8)	0.125	0.125	1.000(14)	0.021(3)
O'	8*b*	0.375	0.375	0.375	1.064(18)	0.026(7)
50% Sb Pyrochlore: *a* = 10.29167(11) Å / Crystallite Size = 13.2 ± 1.4 nm						
Ca	16*d*	0.5	0.5	0.5	0.610(3)	0.0568(8)
Na	16*d*	0.5	0.5	0.5	0.356(5)	0.0568(8)
Ir	16*c*	0	0	0	0.467(2)	0.0149(2)
Sb	16*c*	0	0	0	0.533(2)	0.0149(2)
O	48*f*	0.3277(2)	0.125	0.125	1.002(5)	0.0092(9)
O'	8*b*	0.375	0.375	0.375	1.001(7)	0.067(3)
100% Sb Pyrochlore: *a* = 10.3214(2) Å / Crystallite Size = 16.5 ± 2.1 nm						
Ca	16*d*	0.5	0.5	0.5	0.621(4)	0.0181(11)
Na	16*d*	0.5	0.5	0.5	0.336(7)	0.0181(11)
Sb	16*c*	0	0	0	1.000(1)	0.0111(2)
O	48*f*	0.3323(4)	0.125	0.125	1.000(8)	0.0145(19)
O'	8*b*	0.375	0.375	0.375	1.010(9)	0.065(7)

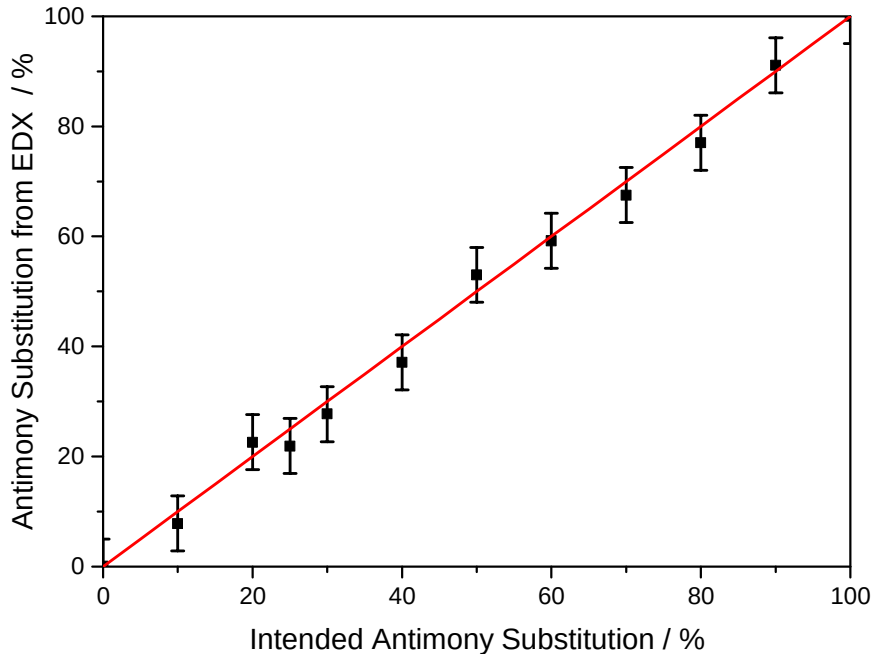

Figure S2.1.2: Measured antimony content from EDXA as a function of intended antimony substitution.

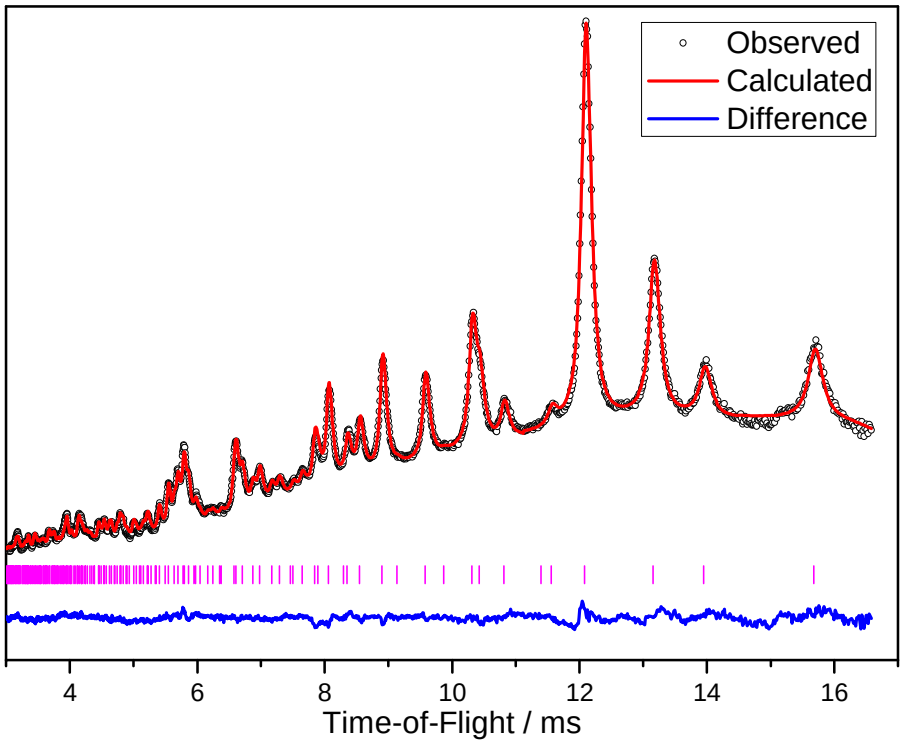

Figure S2.1.3: Rietveld refinement against time-of-flight neutron data from bank 5 of GEM for 50 % antimony substituted calcium sodium iridium oxide.

Table 2.1.2: Structural details of 50 % antimony substituted calcium sodium iridium oxide, obtained from Rietveld refinement of powder neutron diffraction data.

Atom	Site	*x*	*y*	*z*	Occ	U_{iso} / Å^2
50 % Sb Substituted Pyrochlore: *a* = 10.2749(2) Å						
Ca	16*d*	0.5	0.5	0.5	0.589(7)	0.0212(7)
Na	16*d*	0.5	0.5	0.5	0.324(10)	0.0212(7)
Ir	16*c*	0	0	0	0.489(5)	0.00899(16)
Sb	16*c*	0	0	0	0.511(5)	0.00899(16)
O	48*f*	0.32355(10)	0.125	0.125	1.000(2)	0.0099(11)
O'	8*b*	0.375	0.375	0.375	1.000(6)	0.0367(10)
H	32*e*	0.3289	0.3289	0.3289	0.334(12)	*

* U11 = 0.752(2), U22 =0.303(2) , U33 = 0.753(2), U12 = -0.253(3), U13 = -0.400(12), U23= -0.253(3)

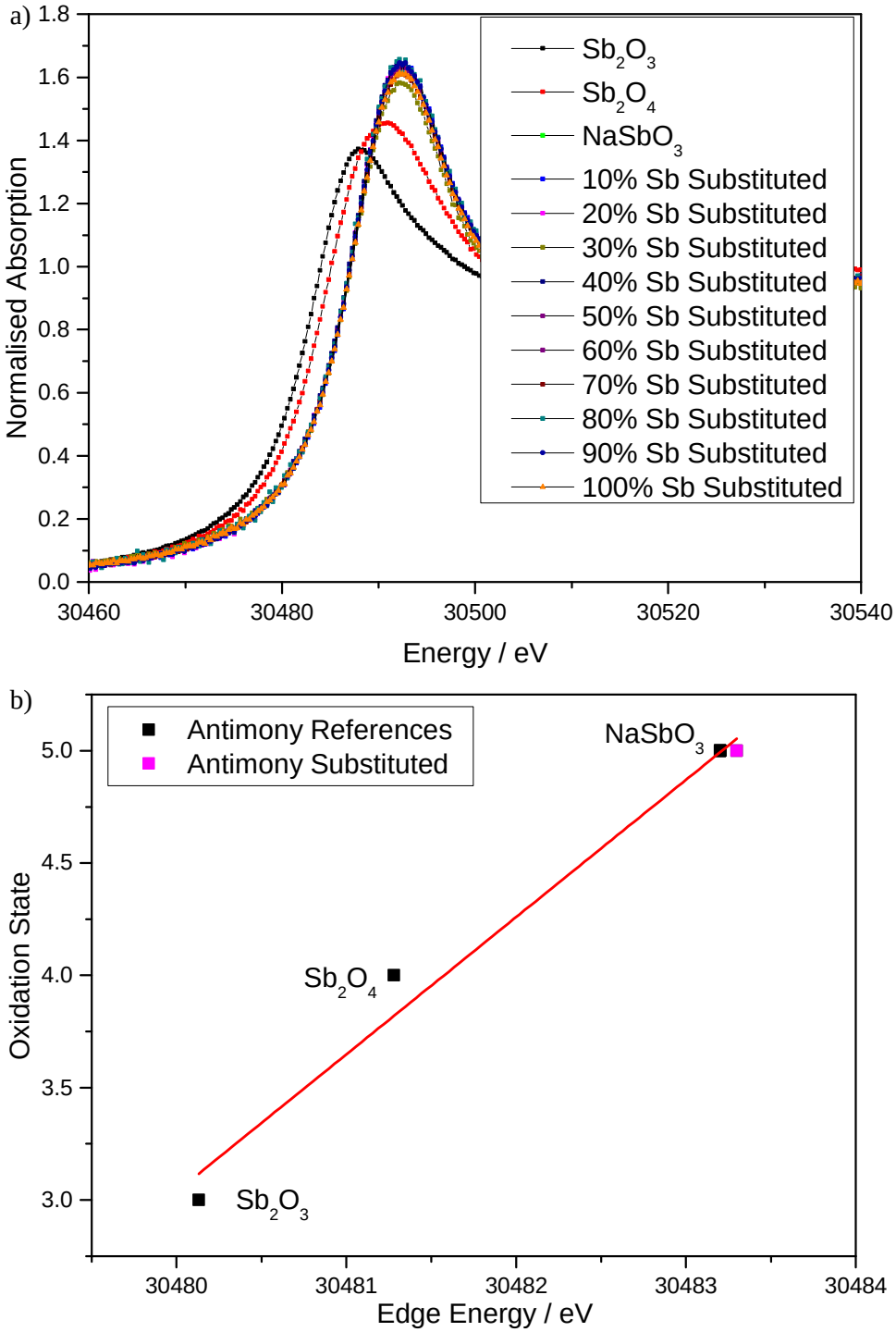

Figure 2.1.4: a) Sb K-edge XANES spectra of antimony calcium sodium iridium antimony oxide materials and reference materials for calibration. b) Edge position against antimony oxidation state.

S2.2 Zirconium substitution

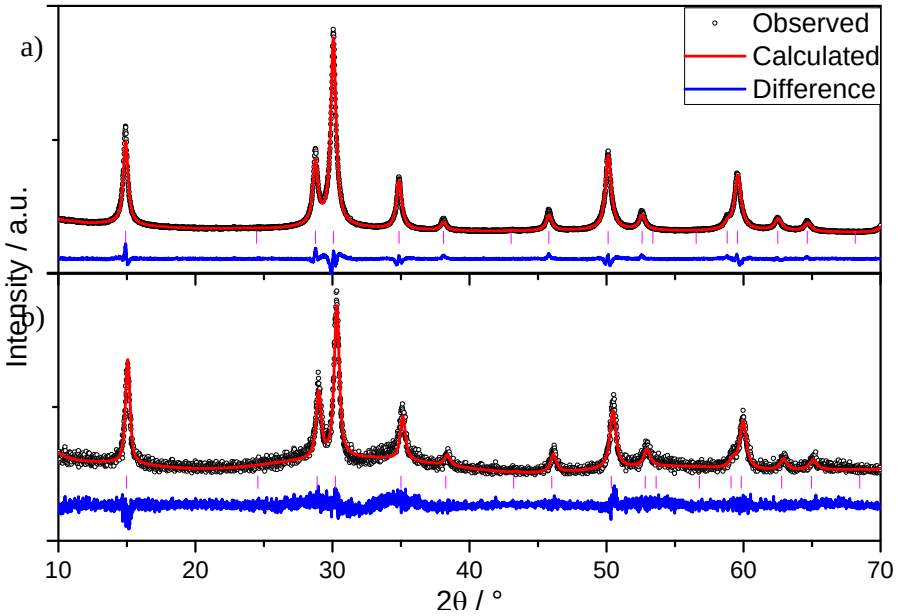

Figure S2.2.1: Rietveld refinements against powder XRD (λ = 1.54056 Å), for $(Ca,Na)_{2-x}(Ir_{1-y}Zr_y)_2O_6{\cdot}H_2O$, a) y = 0.25 and b) y = 0.50.

Table S2.2.1: Structural details of pyrochlores obtained from Rietveld refinement of powder XRD data of Zr substituted materials.

Atom	Site	*x*	*y*	*z*	Occ	U_{iso} / Å^2
25 % Zr Pyrochlore: *a* = 10.2471(5) Å / Crystallite Size = 15.4 ± 1.8 nm						
Ca	16*d*	0.5	0.5	0.5	0.594(13)	0.24(4)
Na	16*d*	0.5	0.5	0.5	0.24(2)	0.24(4)
Zr	16*d*	0.5	0.5	0.5	0.061(6)	0.24(4)
Ir	16*c*	0	0	0	0.795(3)	0.082(6)
Zr	16*c*	0	0	0	0.205(5)	0.082(6)
O	48*f*	0.3236(14)	0.125	0.125	0.99(2)	0.16(7)
O'	8*b*	0.375	0.375	0.375	1.00(5)	0.40(18)
50 % Zr Pyrochlore: *a* = 10.26542(11) Å / Crystallite Size = 14.4 ± 1.5 nm						
Ca	16*d*	0.5	0.5	0.5	0.579(3)	0.0315(5)
Na	16*d*	0.5	0.5	0.5	0.300(5)	0.0315(5)
Zr	16*d*	0.5	0.5	0.5	0.120(1)	0.0315(5)
Ir	16*c*	0	0	0	0.560(1)	0.0226(2)
Zr	16*c*	0	0	0	0.440(1)	0.0226(2)
O	48*f*	0.3328(2)	0.125	0.125	1.001(5)	0.0286(14)
O'	8*b*	0.375	0.375	0.375	0.998(6)	0.076(5)

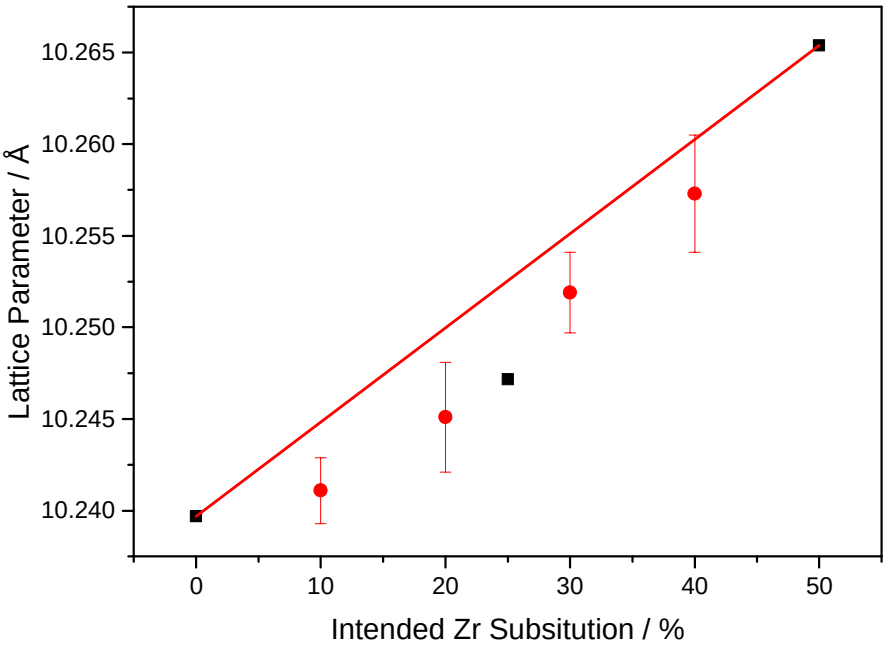

Figure S2.2.2: Refined lattice parameter as a function of intended zirconium substitution. Black points from Rietveld fits and red points from Le Bail fits. Red line is an extrapolation between the two extremes in composition.

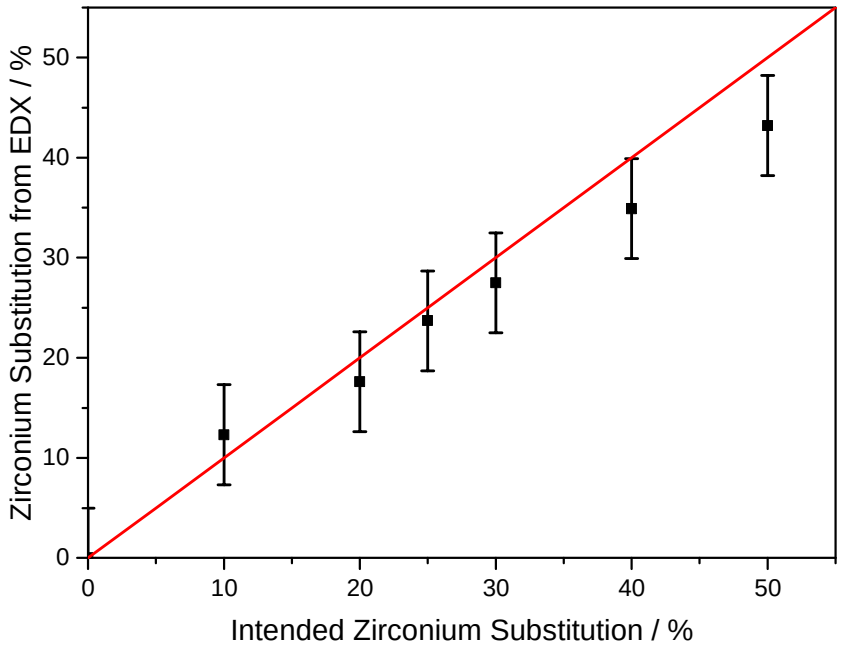

Figure S2.2.3: Measured zirconium content from EDX as a function of intended zirconium substitution.

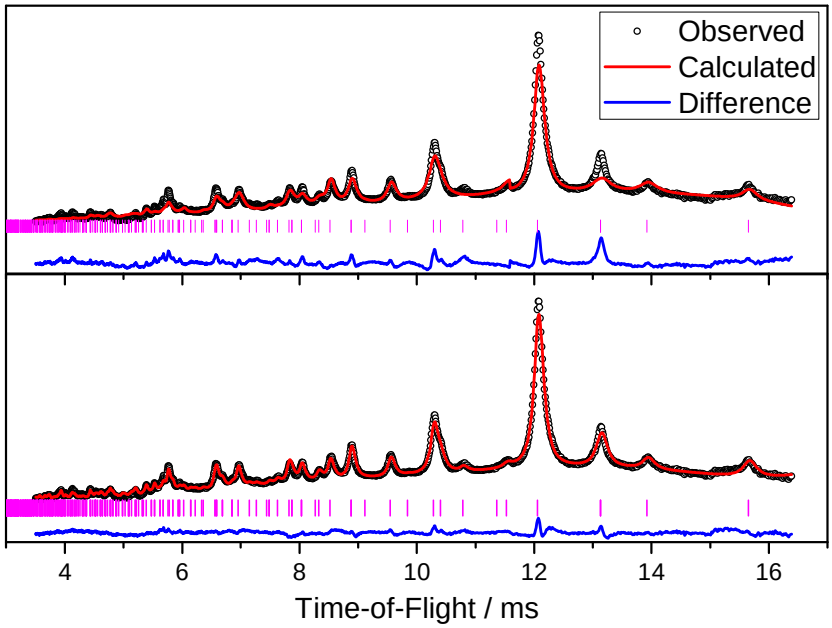

Figure S2.2.4: Rietveld refinements against time-of-flight neutron data from bank 5 of GEM for 50 % zirconium substituted calcium sodium iridium oxide. a) With all zirconium on 16*c* site. b) With a small fraction of zirconium on 16*d* site.

Table S2.2.2: Structural details of 50 % zirconium substituted calcium sodium iridium oxide pyrochlore obtained from Rietveld refinement of powder neutron diffraction data.

Atom	Site	*x*	*y*	*z*	Occ	U_{iso} / Å^2
50 % Zr Substituted Pyrochlore: *a* = 10.2318(3) Å						
Ca	16*d*	0.5	0.5	0.5	0.568(11)	0.0243(10)
Na	16*d*	0.5	0.5	0.5	0.315(15)	0.0243(10)
Zr	16d	0.5	0.5	0.5	0.120(7)	0.0243(10)
Ir	16*c*	0	0	0	0.560(3)	0.0095(2)
Zr	16*c*	0	0	0	0.440(3)	0.0095(2)
O	48*f*	0.3303(2)	0.125	0.125	1.000(3)	0.0152(2)
O'	8*b*	0.375	0.375	0.375	0.965(12)	0.0233(14)
H	32*e*	0.3289	0.3289	0.3289	0.48(3)	*

* U11 = 0.4342(16), U22 = 0.4342(16), U33 = 0.4342(16), U12 = -0.238(2), U13 = -0.238(2), U23 = -0.238(2)

S2.3 Ruthenium substitution

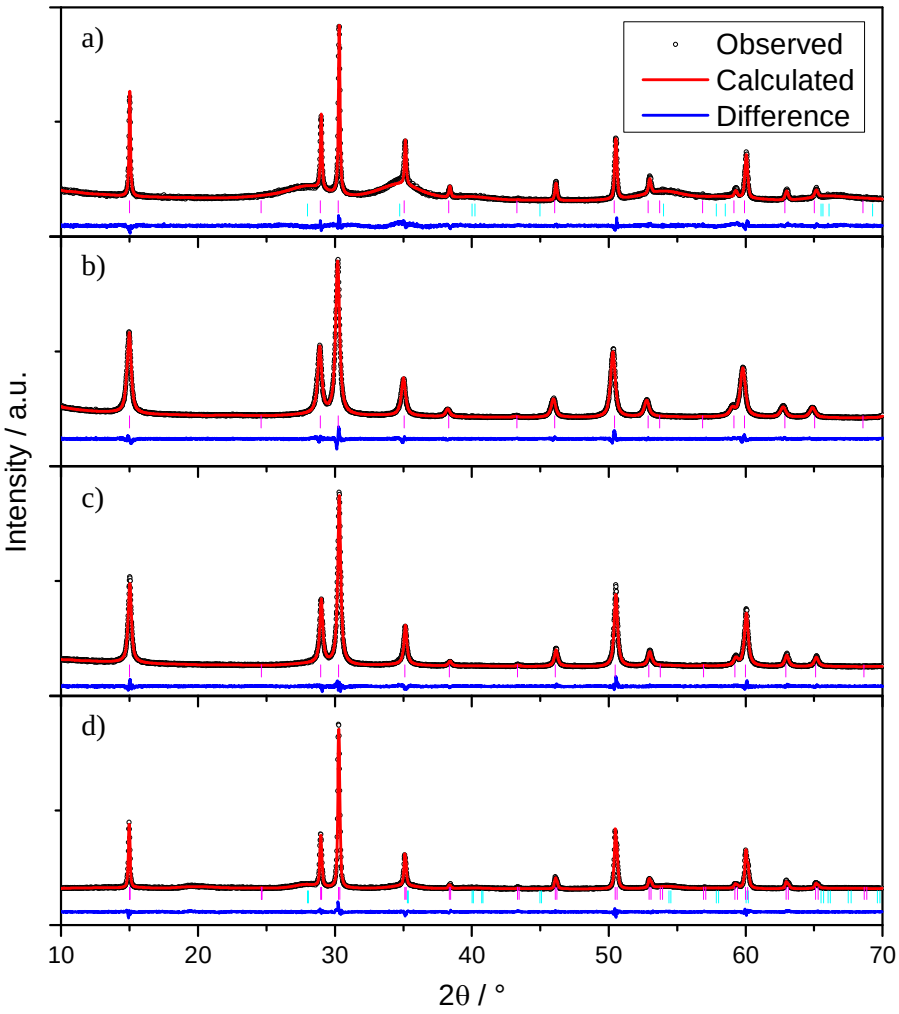

Figure S2.3.1: Rietveld refinements against powder XRD data (λ = 1.54056 Å) for $(Ca,Na)_{2-x}(Ir_{1-y}Ru_y)_2O_6 \cdot H_2O$, a) y = 0.25, b) y = 0.50, c) y = 0.75 and d) y = 1.00.

Table S2.3.1: Structural details of pyrochlores obtained from Rietveld refinement of powder XRD data, of ruthenium substituted materials.

Atom	Site	*x*	*y*	*z*	Occ	U_{iso} / Å^2
25 % Ru Pyrochlore: a = 10.23528(8) Å / Crystallite Size = 35.2 ± 10.0 nm						
Ca	16*d*	0.5	0.5	0.5	0.637(5)	0.020(2)
Na	16*d*	0.5	0.5	0.5	0.362(9)	0.020(2)
Ir	16*c*	0	0	0	0.748(3)	0.0164(4)
Ru	16*c*	0	0	0	0.252(3)	0.0164(4)
O	48*f*	0.3327(7)	0.125	0.125	0.998(13)	0.027(3)
O'	8*b*	0.375	0.375	0.375	1.00(2)	0.012(7)
50 % Ru Pyrochlore: *a* = 10.23414(9) Å / Crystallite Size = 19.2 ± 2.1 nm						
Ca	16*d*	0.5	0.5	0.5	0.669(3)	0.0888(9)
Na	16*d*	0.5	0.5	0.5	0.321(1)	0.0888(9)
Ir	16*c*	0	0	0	0.444(1)	0.0151(2)
Ru	16*c*	0	0	0	0.556(1)	0.0151(2)
O	48*f*	0.3266(3)	0.125	0.125	1.000(5)	0.0053(8)
O'	8*b*	0.375	0.375	0.375	1.001(11)	0.018(3)
75 % Ru Pyrochlore: *a* = 10.22500(7) Å / Crystallite Size = 25.9 ± 2.2 nm						
Ca	16*d*	0.5	0.5	0.5	0.619(2)	0.0150(7)
Na	16*d*	0.5	0.5	0.5	0.325(4)	0.0150(7)
Ir	16*c*	0	0	0	0.229(1)	0.0131(6)
Ru	16*c*	0	0	0	0.771(1)	0.0131(6)
O	48*f*	0.3239(3)	0.125	0.125	1.000(5)	0.0017(9)
O'	8*b*	0.375	0.375	0.375	1.001(11)	0.025(3)
100 % Ru Pyrochlore: *a* = 10.22067(9) Å / Crystallite Size = 50.4 ± 3.7 nm						
Ca	16*d*	0.5	0.5	0.5	0.651(4)	0.0443(6)
Na	16*d*	0.5	0.5	0.5	0.351(8)	0.0443(6)
Ru	16*c*	0	0	0	1.000(2)	0.0138(4)
O	48*f*	0.3372(5)	0.125	0.125	1.000(9)	0.041(2)
O'	8*b*	0.375	0.375	0.375	1.001(11)	0.045(6)

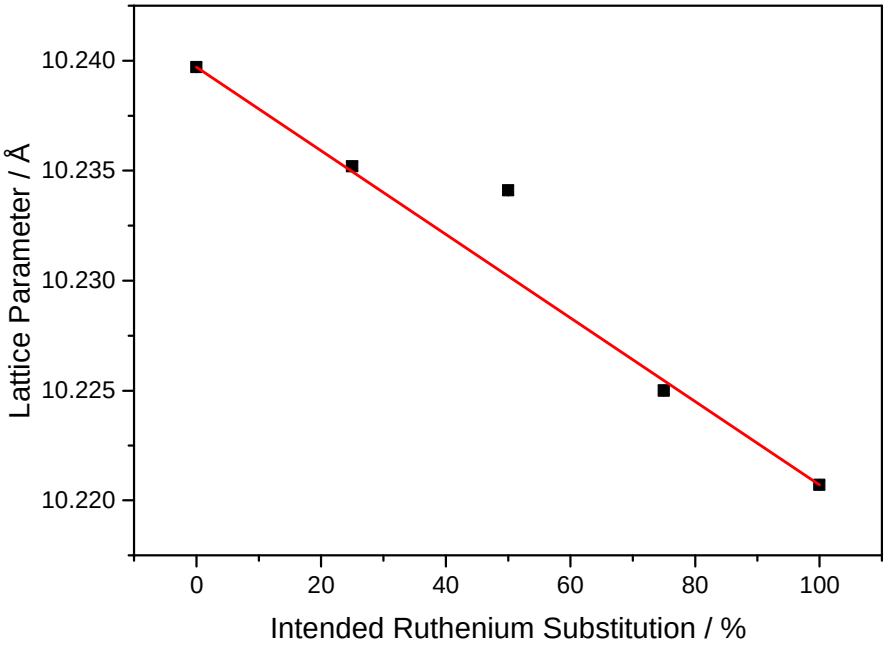

Figure S2.3.2: Refined lattice parameter as a function of intended ruthenium substitution.

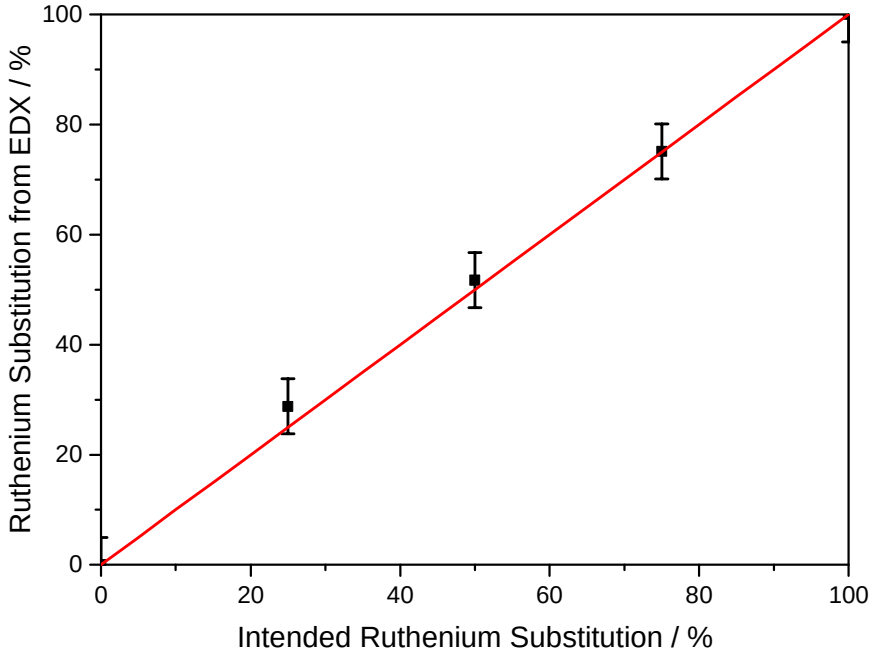

Figure S2.3.3: Measured ruthenium content from EDX as a function of nominal ruthenium substitution.

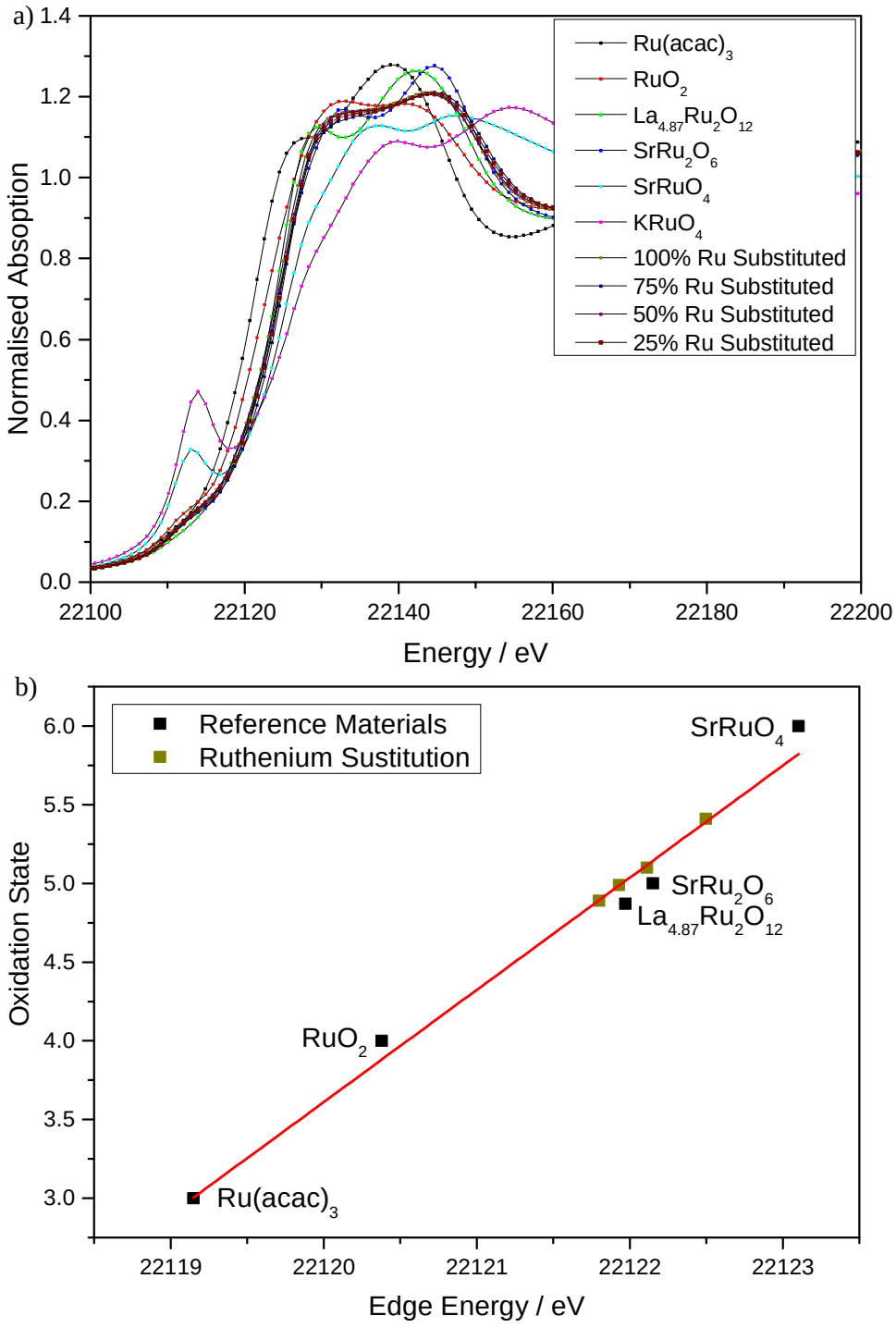

Figure S2.3.4: a) Ru K-edge XANES spectra of ruthenium substituted pyrochlore materials and reference materials for calibration. b) Edge Position against ruthenium oxidation state.

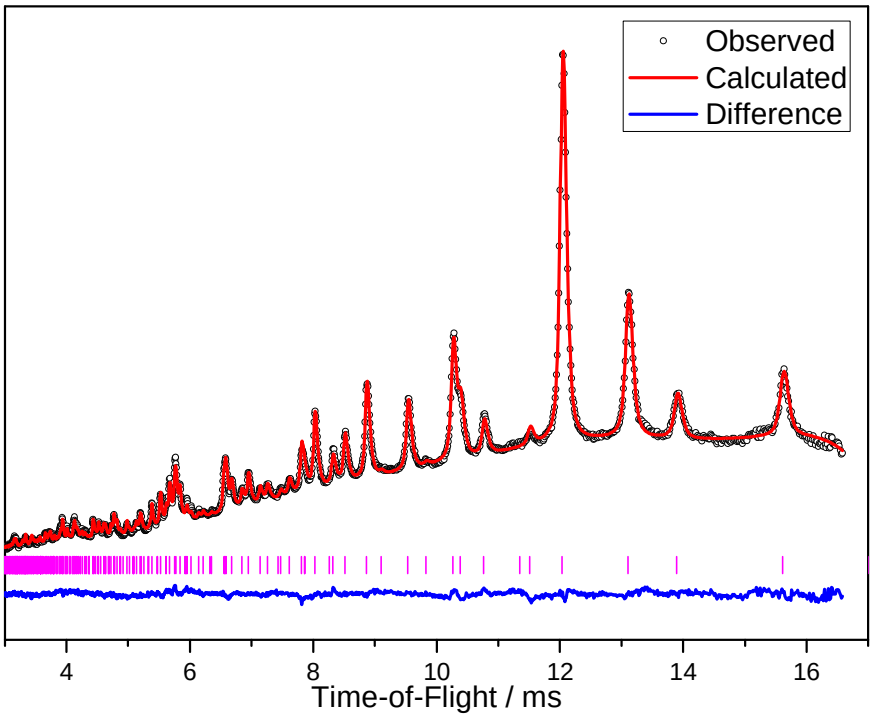

Figure S2.3.5: Rietveld refinement against time-of-flight neutron data from bank 5 of GEM for 50 % ruthenium substituted calcium sodium iridium oxide.

Table S2.3.2: Structural details of 50 % ruthenium substituted calcium sodium iridium oxide pyrochlore obtained from Rietveld refinement of powder neutron diffraction data.

Atom	Site	*x*	*y*	*z*	Occ	U_{iso} / Å^2
50 % Ru Substituted Pyrochlore: *a* = 10.23360(17) Å						
Ca	16*d*	0.5	0.5	0.5	0.594(5)	0.0310(8)
Na	16*d*	0.5	0.5	0.5	0.320(9)	0.0310(8)
Ir	16*c*	0	0	0	0.496(6)	0.00726(5)
Ru	16*c*	0	0	0	0.504(6)	0.00726(5)
O	48*f*	0.32304(10)	0.125	0.125	1.000(2)	0.1072(12)
O'	8*b*	0.375	0.375	0.375	0.990(6)	0.0280(9)
H	32*e*	0.3289	0.3289	0.3289	0.495(13)	*

* U11 = 0.7970(9), U22 = 0.3669(9) , U33 = 0.7970(9), U12 = -0.2911(7), U13 = -0.3972(7), U23 = -0.2911(7)

S2.4: Rhodium Substitution

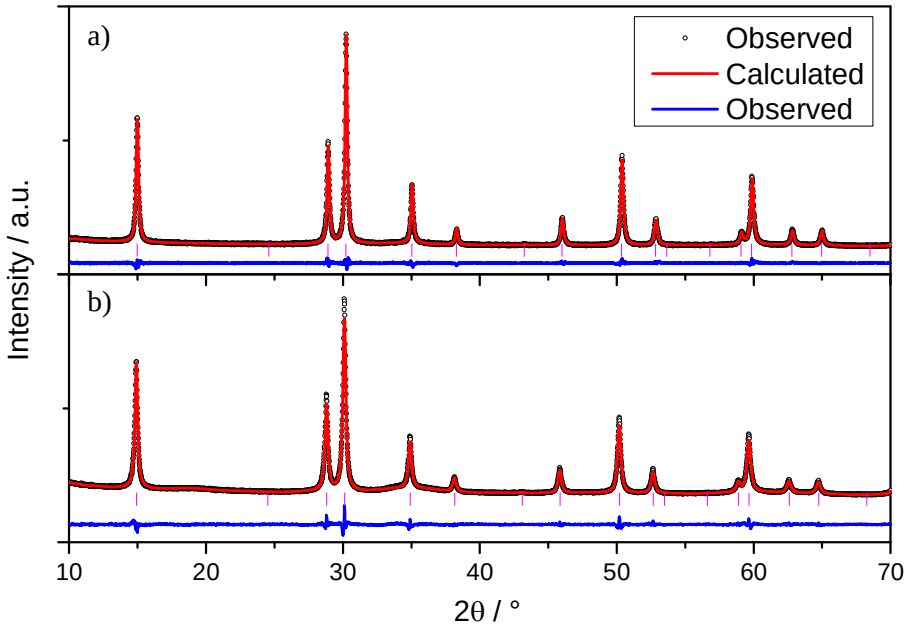

Figure S2.4.1: Rietveld refinements against powder XRD data (λ = 1.54056 Å) for $(Ca,Na)_{2-x}(Ir_{1-y}Rh_y)_2O_6 \cdot H_2O$, a) y = 0.15 and b) y = 0.3.

Table S2.4.1: Structural details of pyrochlores obtained from Rietveld refinement of powder XRD data, of Rh substituted materials.

Atom	Site	*x*	*y*	*z*	Occ	U_{iso} / Å^2
15 % Rh Pyrochlore: *a* = 10.24467(5) Å / Crystallite Size = 32.4 ± 3.5 nm						
Ca	16*d*	0.5	0.5	0.5	0.630(3)	0.0327(9)
Na	16*d*	0.5	0.5	0.5	0.352(6)	0.0327(9)
Ir	16*c*	0	0	0	0.830(2)	0.0109(2)
Rh	16*c*	0	0	0	0.170(2)	0.0109(2)
O	48*f*	0.3284(3)	0.125	0.125	1.000(6)	0.0119(14)
O'	8*b*	0.375	0.375	0.375	1.001(8)	0.018(3)
30 % Rh Pyrochlore: *a* = 10.27437(7) Å / Crystallite Size = 25.8 ± 2.2 nm						
Ca	16*d*	0.5	0.5	0.5	0.594(3)	0.0304(9)
Na	16*d*	0.5	0.5	0.5	0.269(5)	0.0304(9)
Ir	16*c*	0	0	0	0.707(2)	0.0165(2)
Rh	16*c*	0	0	0	0.293(2)	0.0165(2)
O	48*f*	0.3280(3)	0.125	0.125	1.000(6)	0.0268(15)
O'	8*b*	0.375	0.375	0.375	1.000(8)	0.038(4)

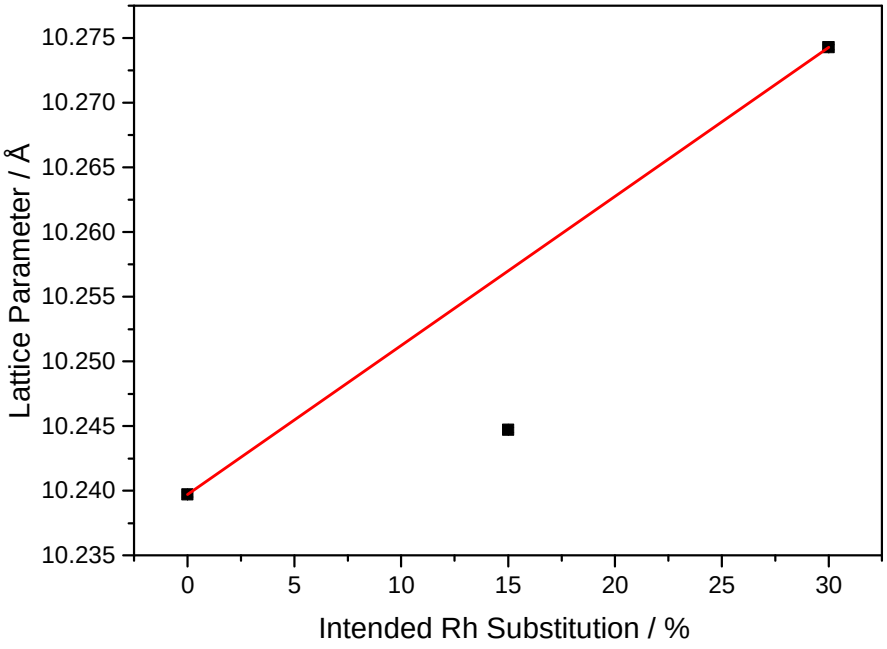

.

Figure S2.4.2: Refined Lattice Parameter as a function of intended rhodium substitution.

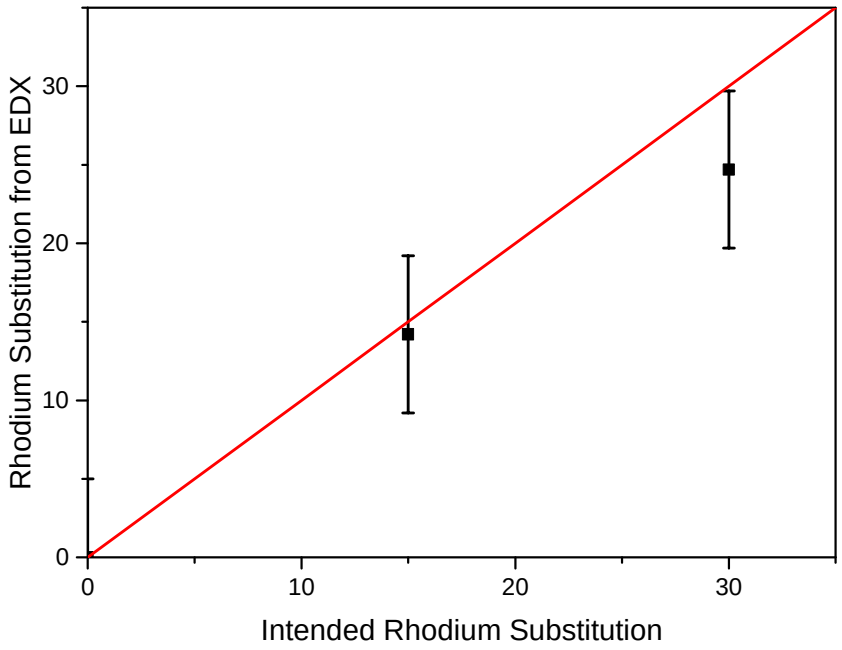

Figure S2.4.3: Measured rhodium content from EDX as a function of nominal rhodium substitution.

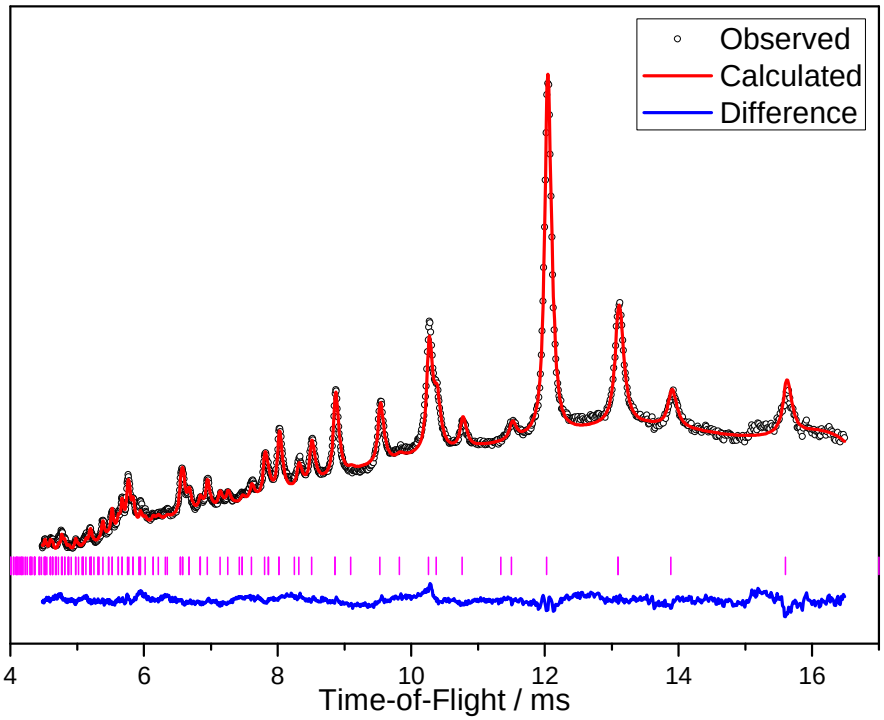

Figure S2.4.4: Rietveld refinements against time-of-flight neutron data from bank 5 of GEM for 30 % rhodium substituted calcium sodium iridium oxide.

Table S2.4.2: Structural details of 30 % rhodium substituted calcium sodium iridium oxide pyrochlore obtained from Rietveld refinement of powder neutron diffraction data.

Atom	Site	*x*	*y*	*z*	Occ	U_{iso} / Å^2
30 % Rh Substituted Pyrochlore: *a* = 10.2263(2) Å						
Ca	16*d*	0.5	0.5	0.5	0.571(10)	0.0267(12)
Na	16*d*	0.5	0.5	0.5	0.303(13)	0.0267(12)
Ir	16*c*	0	0	0	0.729(7)	0.0096(2)
Rh	16*c*	0	0	0	0.271(7)	0.0096(2)
O	48*f*	0.3229(2)	0.125	0.125	1.000(3)	0.0123(2)
O'	8*b*	0.375	0.375	0.375	0.999(10)	0.0238(12)
H	32*e*	0.3289	0.3289	0.3289	0.50(2)	*

* U11 = 0.659(14), U22 = 0.659(14) , U33 = 0.659(14), U12 = -0.327(7), U13 = -0.327(7), U23= -0.327(7)

S3: Samples prepared at lower temperature and lower pH

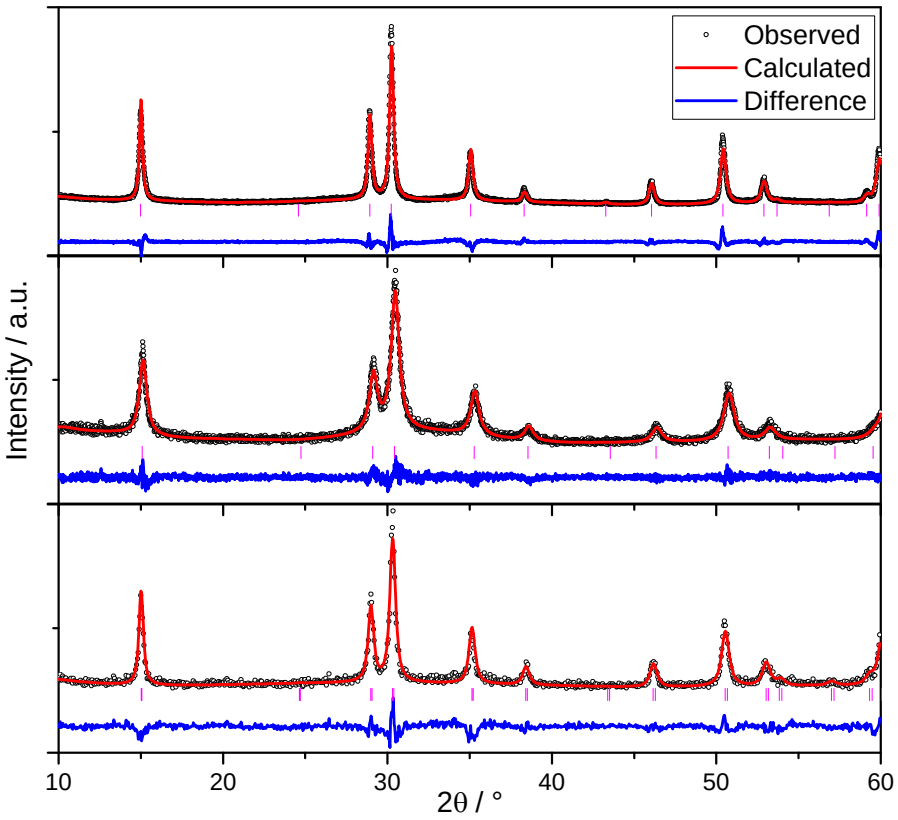

Figure S3.1: Le Bail fits to powder XRD data (λ = 1.54056 Å) from $(Ca,Na)_{2-x}Ir_2O_6{\cdot}nH_2O$ materials produced, a) in 5 M NaOH at 240 °C, b) in 10 M NaOH at 170 °C, and c) in 10 M NaOH at 200 °C**.**

Table S3.1: Effect of reaction conditions on lattice parameter and crystallite size of $(Ca,Na)_{2-x}Ir_2O_6{\cdot}H_2O$, determined from laboratory powder X-ray diffraction. For comparison the standard material prepared at 240 °C in 10 M is also shown here.

Synthesis Temperature / °C	NaOH Concentration / M	Lattice Parameter / Å	Scherrer crystallite Size / nm
170	10	10.1981(11)	11.2 ± 1.9
200	10	10.2142(5)	25.0 ± 0.7
240	10	10.23978(5)	36.2 ± 2.4
240	5	10.2355(2)	20.8 ± 4.4

S4 TEM

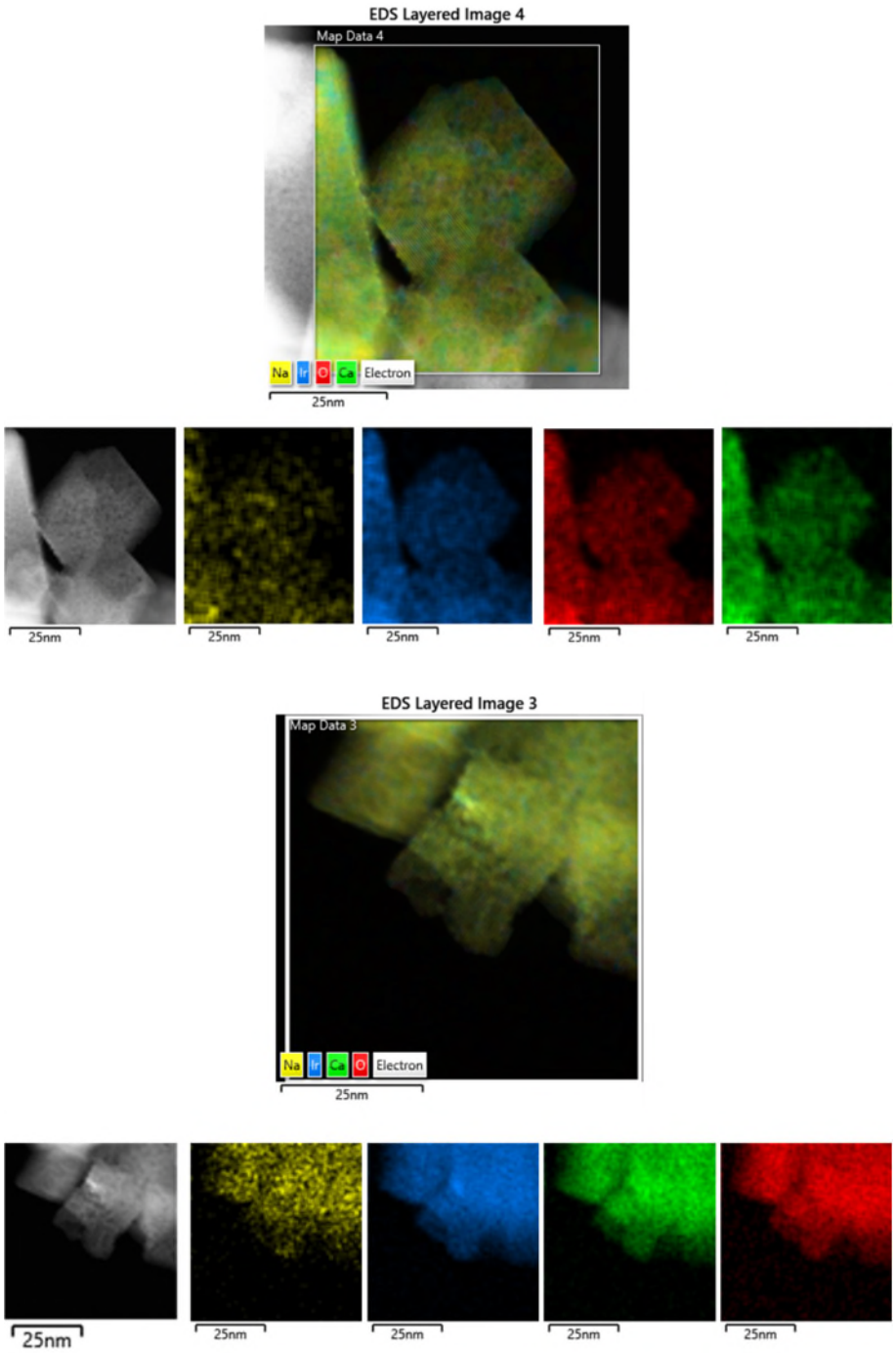

Figure S4.1: EDS maps of $(Na,Ca)_{2-x}Ir_2O_6.nH_2O$ showing two regions of the sample.

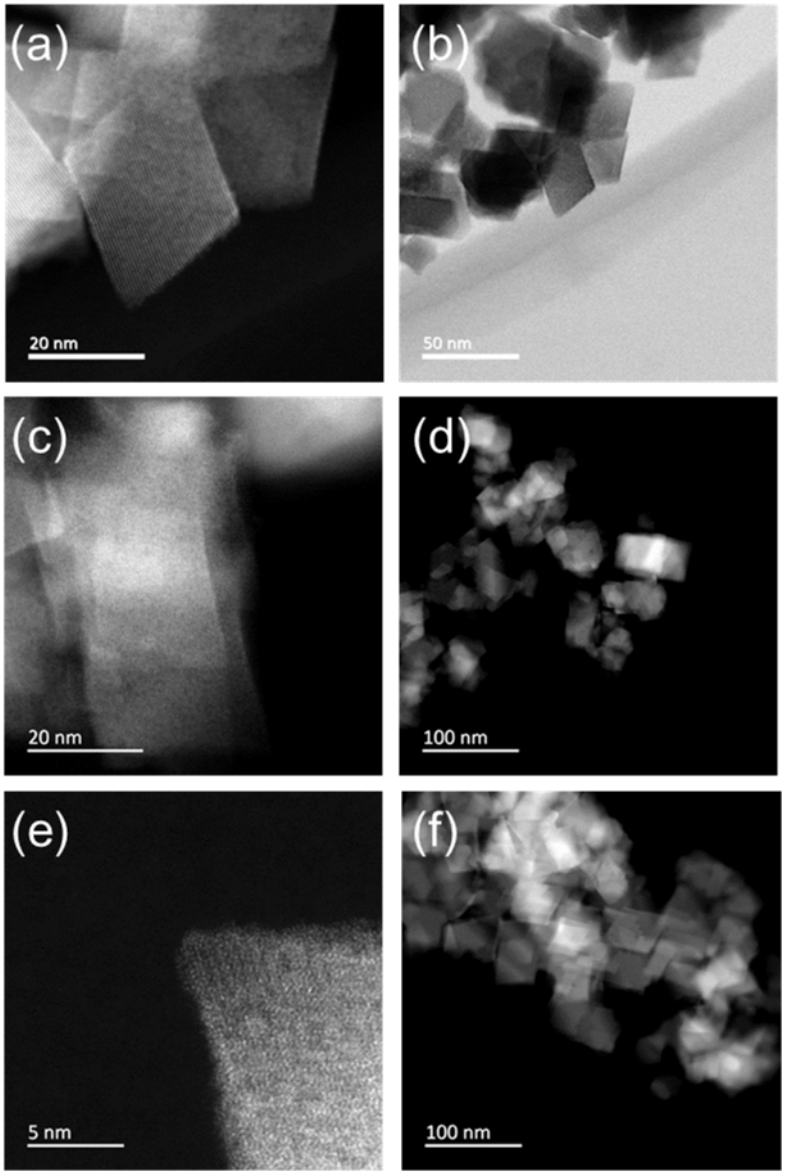

Figure S4.2: TEM images of $(Na,Ca)_{2-x}Ir_2O_6.nH_2O$ (a) and (b) as-made, (c) and (d) after 80 °C acid treatment and (e) and (f) after 100 °C acid treatment.

S5 Acid leached samples

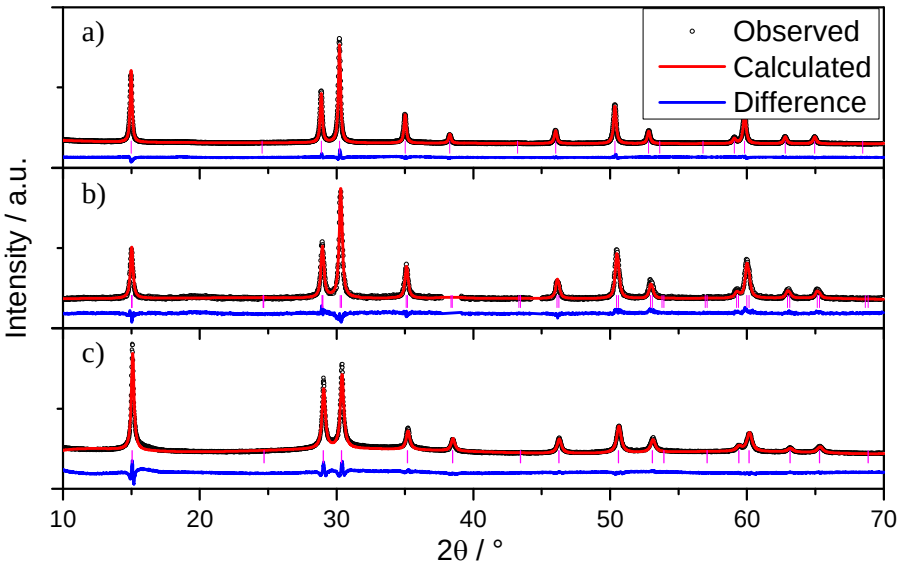

Figure S5.1: Rietveld refinements against powder XRD data (λ = 1.54056 Å) for $Ca_{2-x}Ir_2O_6 \cdot H_2O$, a) as made, a = 10.24030(3) Å, b) leached at 80 °C, a = 10.2194(2) Å, c) leached at 110 °C, a =10.19599(12) Å.

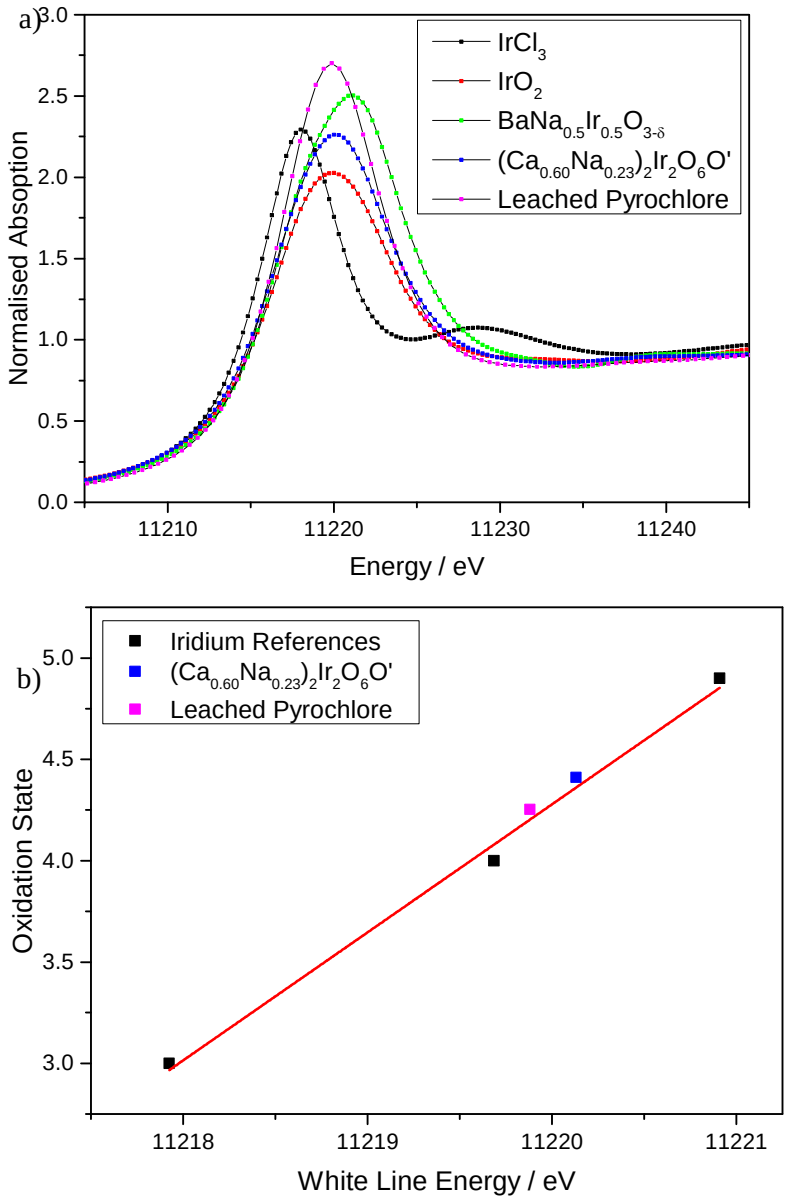

Figure S5.2: a) Ir L_{III}-edge XANES spectra of calcium sodium iridium oxide acid leached at 110 °C and reference materials for calibration. b) White line position against iridium oxidation state.

Table S5.1: Surface areas and oxygen evolution onset voltages at the beginning and end of life for calcium iridium oxide and calcium sodium iridium oxide pyrochlore materials under various degrees of acid leaching.

Material / Leaching Temperature	BET	OER Onset Voltage / V	
	Surface Area / m^2g^{-1}	Beginning of Life	End of Life
$(Ca,Na)_{2-x}Ir_2O_6O'$ / 80 °C	39.7	1.433	1.429
$(Ca,Na)_{2-x}Ir_2O_6O'$ / 110 °C	22.6	1.407	1.409
$Ca_{2-x}Ir_2O_6O'$	27.3	1.421	1.422
$Ca_{2-x}Ir_2O_6O'$ / 80 °C	30.6	1.422	1.422
$Ca_{2-x}Ir_2O_6O'$ / 110 °C	28.9	1.407	1.412

S6 INS studies

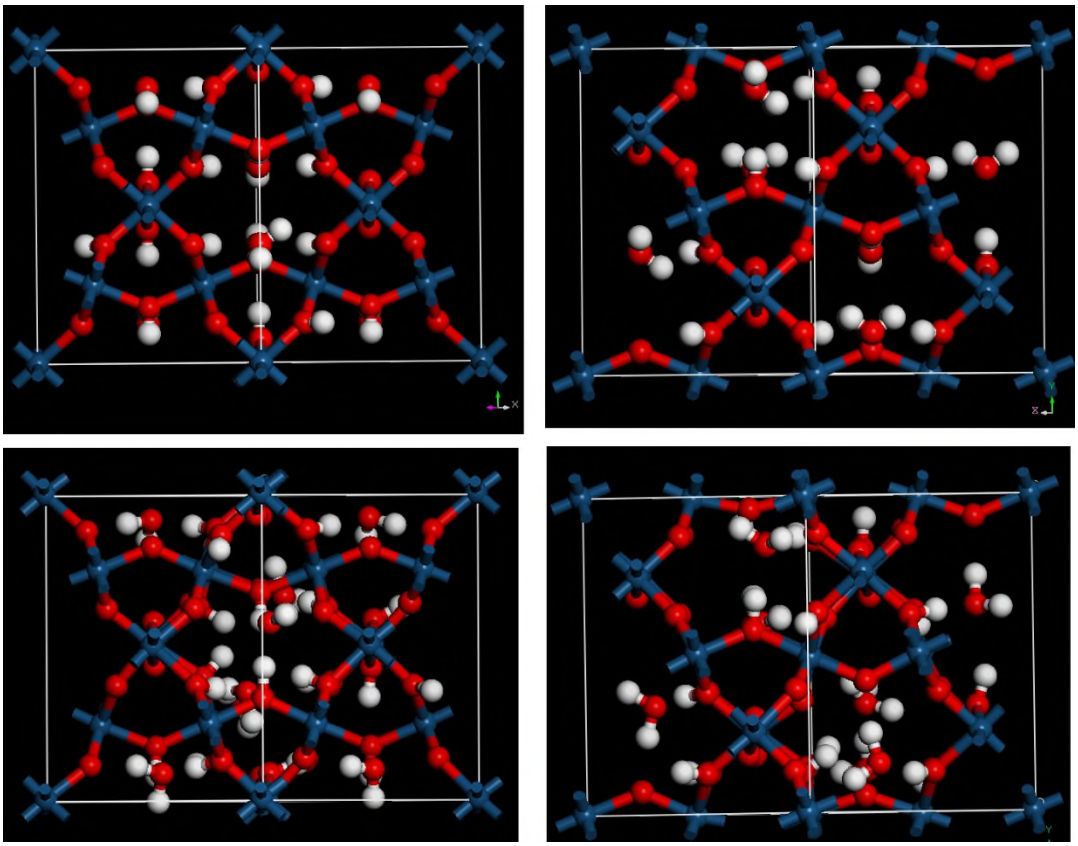

Figure S6.1: Structures of $Ir_2O_4(OH)_2.H_2O$ used for the computational studies. Left side: the ordered model, right side: the disordered model. Top row: initial structures, bottom row: after geometry optimisation.

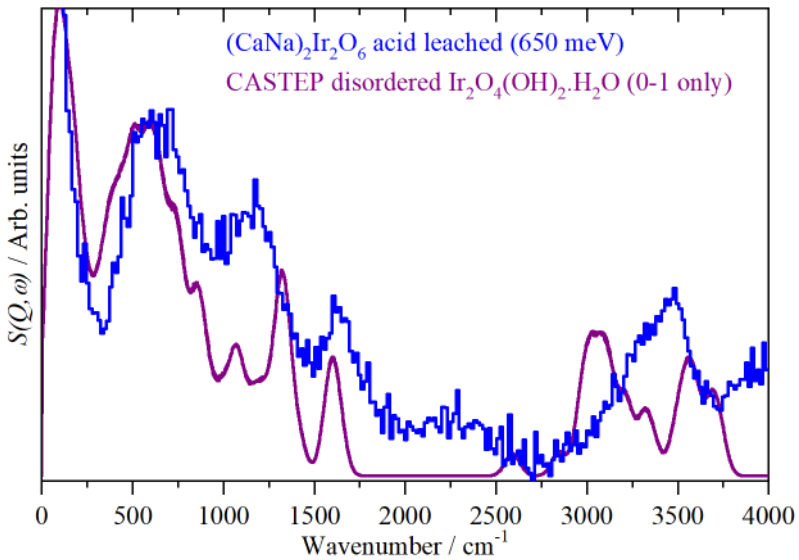

Figure S6.2: Comparison of the INS spectra of acid leached $(Na,Ca)_{2-x}Ir_2O_6.nH_2O$ and that generated from the geometry optimised disordered structure of $Ir_2O_4(OH)_2.H_2O$ (bottom right in Figure S6.1).

Table S6.1: Observed and calculated transition energies (cm^{-1}) for the acid leached iridate, $(Na,Ca)_{2-x}Ir_2O_6.nH_2O$.

Experimental	Ordered structure	Disordered structure	Assignment
		3700	Weakly H-bonded water O–H stretch
		3560	
3470s,br	3560		Hydroxyl O–H stretch
	3310		Water O–H stretch
	2980	3060	Strongly H-bonded hydroxyl O–H stretch
	2300	2600	Strongly H-bonded hydroxyl O–H stretch
1640m	1620	1610	Water H–O–H bend
	1340	1320	Strongly H-bonded hydroxyl in-plane bend
1160s	1070	1070	Hydroxyl in-plane bend
	780		Hydroxyl out-of-plane bend
600s,br	580	550	Water librations

S7: Further electrochemical / mass spectrometry data from devices

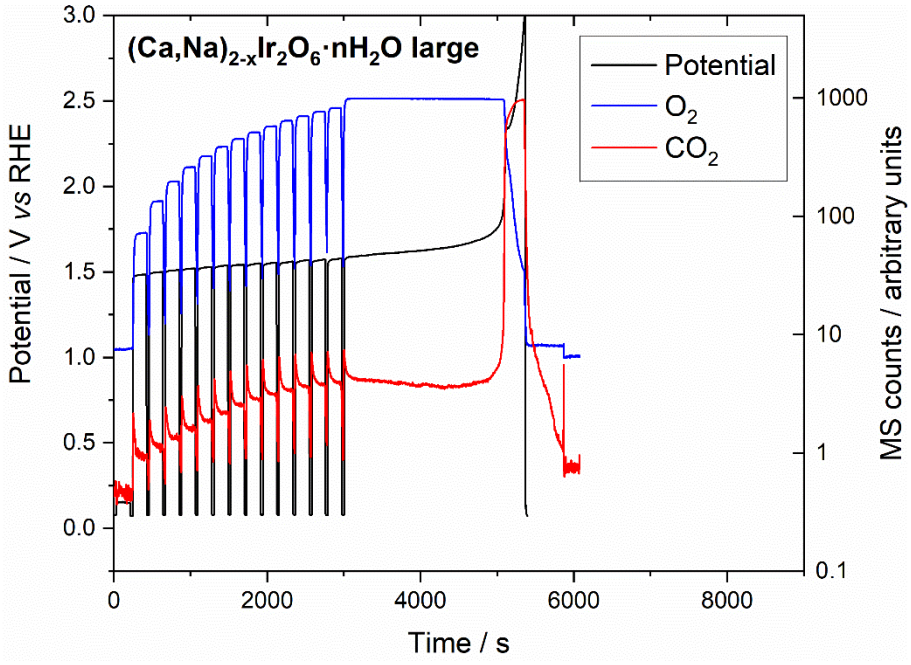

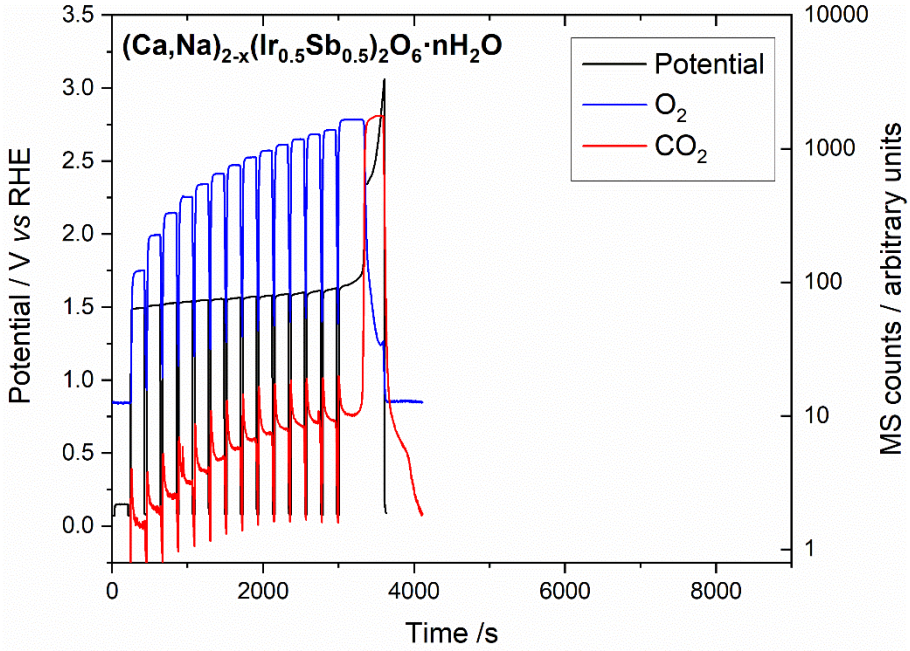
(Ca,Na)2-x(Ir0.5Sb0.5)2O6·nH2O
Potential
O2
CO2
Potential / V vs RHE
MS counts / arbitrary units
Time /s
0.0
0.5
1.0
1.5
2.0
2.5
3.0
3.5
0
2000
4000
6000
8000
1
10
100
1000
10000

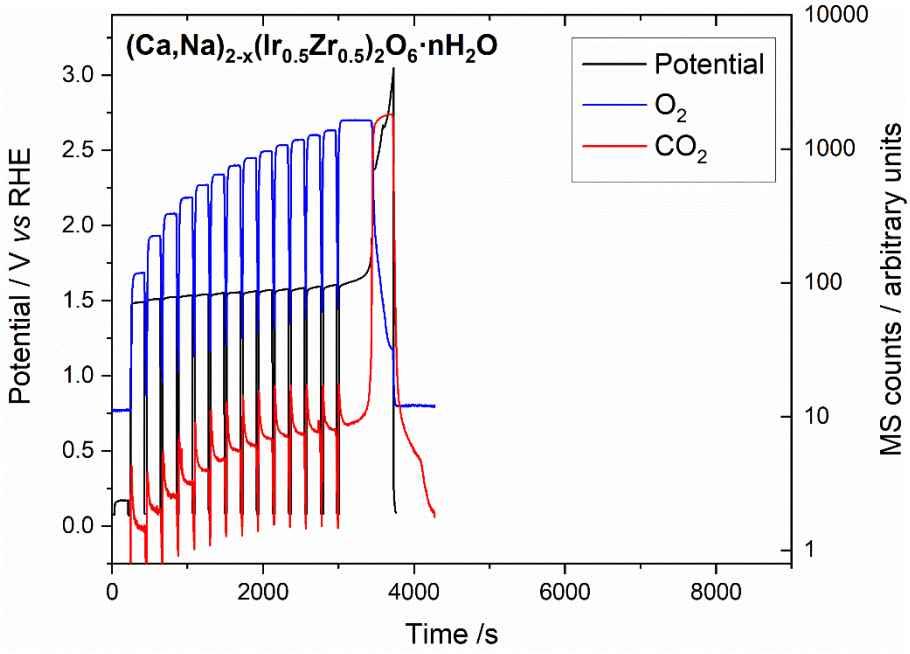
(Ca,Na)2-x(Ir0.5Zr0.5)2O6·nH2O
Potential
O2
CO2
Potential / V vs RHE
MS counts / arbitrary units
Time /s
0.0
0.5
1.0
1.5
2.0
2.5
3.0
0
2000
4000
6000
8000
1
10
100
1000
10000

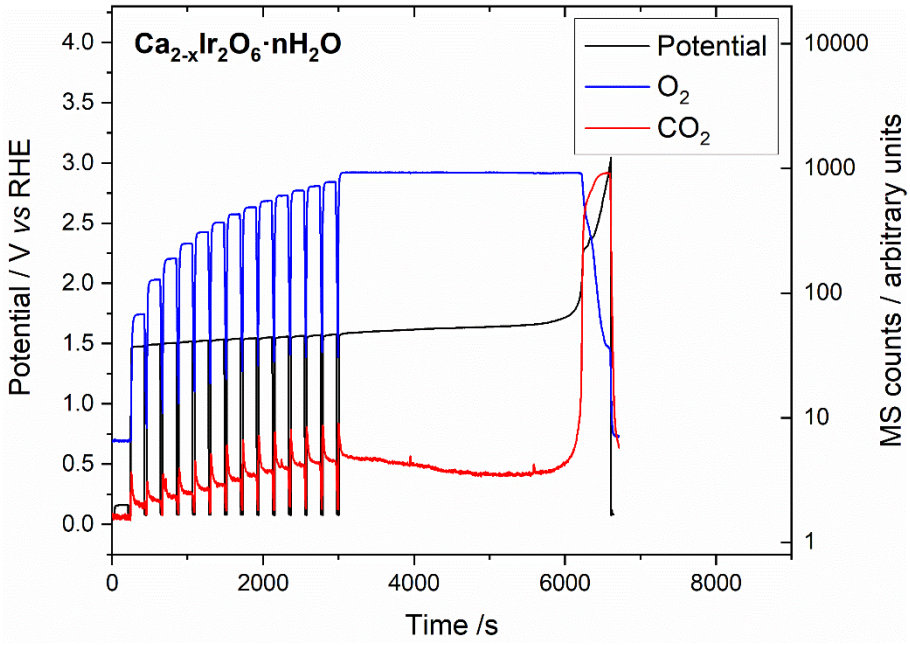
Ca2-xIr2O6·nH2O
Potential
O2
CO2
Potential / V vs RHE
MS counts / arbitrary units
Time /s
4.0
3.5
3.0
2.5
2.0
1.5
1.0
0.5
0.0
10000
1000
100
10
1
0
2000
4000
6000
8000

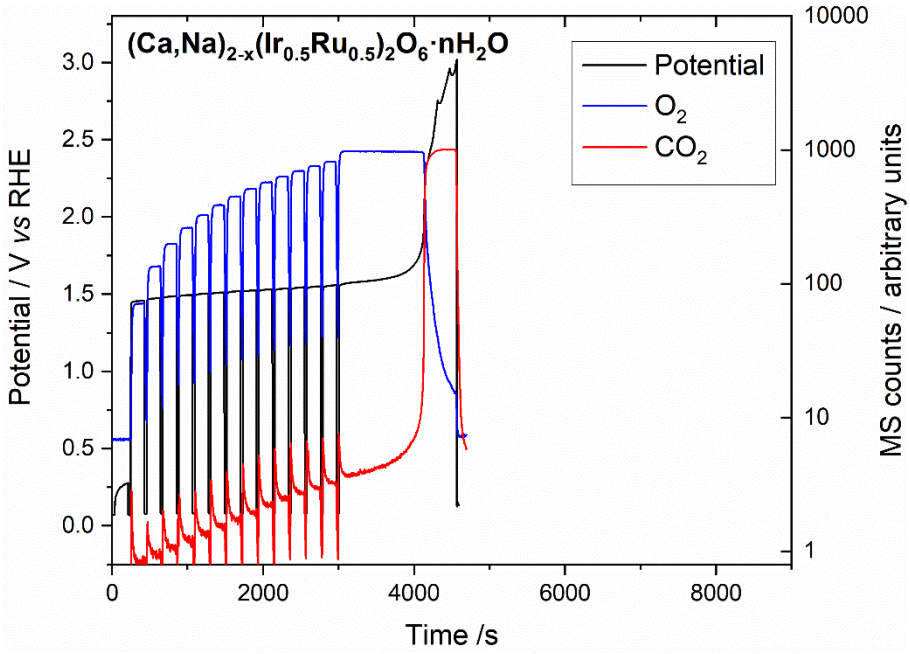
(Ca,Na)2-x(Ir0.5Ru0.5)2O6·nH2O
Potential
O2
CO2
Potential / V vs RHE
MS counts / arbitrary units
Time /s
3.0
2.5
2.0
1.5
1.0
0.5
0.0
10000
1000
100
10
1
0
2000
4000
6000
8000

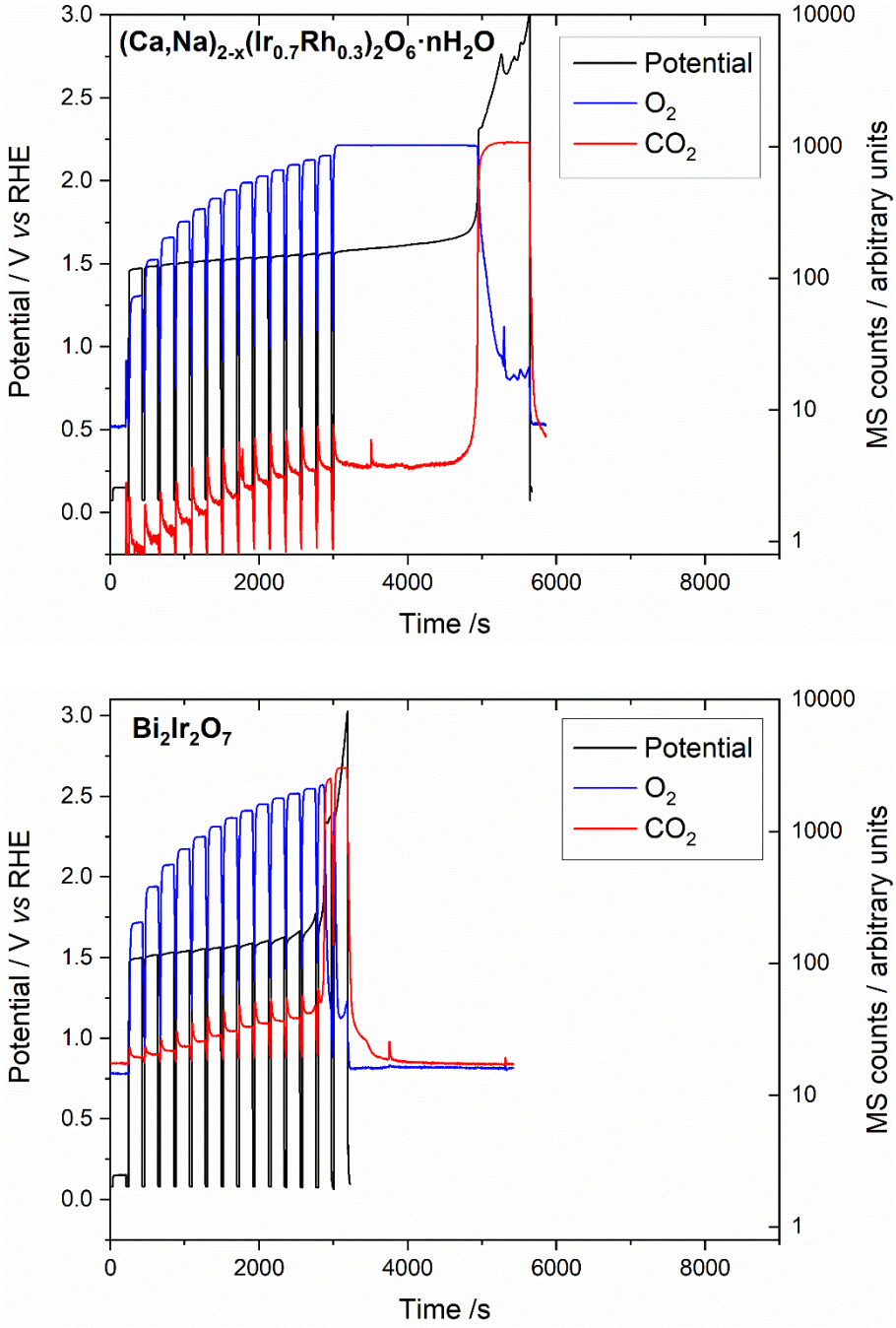

Figure S7.1: Mass spectrometry results as a function of measured potential in devices fabricated from all samples studied (see Figure 3b for data from the small particle size $(Ca,Na)_{2-x}Ir_2O_6{\cdot}nH_2O$)

The O_2:CO_2 ratio provides a direct comparison of the two main competing reactions R1 and R2.

R1) $2H_2O \rightarrow O_2 + 4H^+ + 4e^-$

R2) $C + 2H_2O \rightarrow CO_2 + 4H^+ + 4e^-$

The overall Faradaic Efficiency for $O_2 = \varepsilon_{O2} / (\varepsilon_{CO2} + \varepsilon_{O2})$ where:

ε_{O2} is the calculated Faradaic current for the O_2 evolution reaction

ε_{CO2} is the calculated Faradaic current for the CO_2 evolution reaction

For equivalent mass detection efficiency and the number of electrons yield per gas molecule, an example O_2/CO_2 ratio 100 would yield 100/101 = 99% overall Faradaic Efficiency for O_2 evolution.